Resilience Assessment of Active Distribution Systems Considering Microgrid Formation based on Grid-Edge DERs

Yuxiong Huang[1], Xuanman Rong[1], Gengfeng Li[1], Chen Chen[1], and Zhaohong Bie[1]

[1]Xi'an Jiaotong University

February 13, 2023

Abstract

Distributed energy resources (DERs) provide flexible load restoration strategies, which can effectively enhance the resilience of active distribution systems (ADSs). Whereas, the widespread DERs in ADSs complicate the supply-demand relationship and make the system resilience difficult to access. Therefore, this paper proposes a simulation-based resilience assessment algorithm of ADSs considering the microgrid formation based on grid-edge DERs. Microgrid formation is used to depict the resilience gain of grid-edge DERs on ADSs. Specifically, a resilience assessment framework for ADSs is firstly proposed, where the uncertainty of component state and supply-demand is modelled based on probability statistics. Then the mixed integer linear programming is used to search for optimal load restoration strategies with microgrid formation. On this basis, a set of resilience indices are defined to quantitatively analyse the resilience of ADSs, and a resilience assessment algorithm with uncertainty scenario generation is proposed to obtain these indices. Furthermore, extensive numerical results based on a modified IEEE 123-bus feeder validate the effectiveness of our proposed method.

IET Journals
The Institution of Engineering and Technology

Resilience Assessment of Active Distribution Systems Considering Microgrid Formation based on Grid-Edge DERs

ISSN 1751-8644
doi: 0000000000
www.ietdl.org

Yuxiong Huang[1], Xuanman Rong[1], Gengfeng Li[1], Chen Chen[1], Zhaohong Bie[1]*

[1] *Shaanxi Key Laboratory of Smart Grid, Xi'an Jiaotong University, Xi'an, People's Republic of China*
* *E-mail: gengfengli@xjtu.edu.cn*

Abstract: Distributed energy resources (DERs) provide flexible load restoration strategies, which can effectively enhance the resilience of active distribution systems (ADSs). Whereas, the widespread DERs in ADSs complicate the supply-demand relationship and make the system resilience difficult to access. Therefore, this paper proposes a simulation-based resilience assessment algorithm of ADSs considering the microgrid formation based on grid-edge DERs. Microgrid formation is used to depict the resilience gain of grid-edge DERs on ADSs. Specifically, a resilience assessment framework for ADSs is firstly proposed, where the uncertainty of component state and supply-demand is modelled based on probability statistics. Then the mixed integer linear programming is used to search for optimal load restoration strategies with microgrid formation. On this basis, a set of resilience indices are defined to quantitatively analyse the resilience of ADSs, and a resilience assessment algorithm with uncertainty scenario generation is proposed to obtain these indices. Furthermore, extensive numerical results based on a modified IEEE 123-bus feeder validate the effectiveness of our proposed method.

1 Introduction

Carbon neutrality asks the power distribution system to integrate more renewable distributed energy resources (DERs) e.g. distributed wind turbines and photovoltaic units, promoting distribution systems to active distribution systems (ADSs). The ADS has DERs as a means of managing power grids actively that can improve the resilience efficiently [1]. Meanwhile, it brings some new features to distribution systems, e.g. complicate supply-demand relationship and flexible operation. Notably, the integration of grid-edge DERs enables the ADS to operate with a more resilient fashion [2], that means it can use grid-edge DERs as flexible power units to restore critical loads and reduce power losses when outages come [3].

Grid resilience refers to the capability of enduring and curtailing the adverse impact of disruptions, which comprises three main factors, i.e., absorb, adapt, and recover from extreme events [4]. Resilience assessment quantitatively calculates the capability and further guides the resilience optimization of distribution systems [5]. In recent years, the resilience enhancement of distribution systems considering considering microgrid formation based on grid-edge DERs has become a research hotspot [6]. The influence of loads and DERs on the outage management during the resilient operation of microgrids was analysed in [7]. Mishra et al. [1] studied the vulnerability modelling methods and the restoration measures of power grids under the extreme weather. At the same time, the dynamic boundary microgrid formation provides flexible load restoration strategies [8]. Panteli et al. [9] put forward a general research framework for power system resilience assessment and enhancement. Chen et al. [3] earlier proposed the post-disaster resilient operation model of distribution systems considering microgrids, and modelled the critical load restoration problem of resilient distribution systems as a mixed integer linear programming problem. Wang et al. [10] proposed an optimal decision-making method for multi-timestep load restoration of power distribution systems based on multi-source cooperation. In addition, existing studies also consider the influence of distribution system topology reconstruction [11], distribution system linear topology constraints [12], energy storage equipment and demand side management [13], hierarchical fault management [8]. Bian et al. [14] proposed an restoration model considering the coordination with damage assessment. Huang et al. [15] formulated the microgrid formation problem as a Markov decision process and used the deep Q-network to search for optimal microgrid formation strategies.

The application of resilient planning and operation can be facilitated with the resilience assessment and associated indices. The assessment methods are diverse. For example, Carlson et al. [16] provided frameworks for system-level and regional-level resilience overview using investigation, and a scoring matrix was formulated in [17] to evaluate the system function from different perspectives. Besides, the simulation-based methods were most widely used to analyse the disaster consequences, combined with the disaster scenarios, e.g., in [18] and [19], the power flow analysis was adopted, and in [20], the complex network model was adopted. For systems that have accumulated historical natural disaster, outage and restoration records can be used for data-based reliability analysis [21, 22]. Notably, the existing assessment methods are not fully applicable to the impact of microgrid formation based on edge-grid DERs. Moreover, traditionally, the resilience assessment of the power system focuses on the random component faults, but the optimal load restoration strategies through the microgrid formation has been neglected to make the computational load affordable.

This paper takes into consideration the load restoration through microgrid formation in the resilience assessment process and focuses on the impact of grid-edge DERs on the resilience of ADSs. Firstly, based on the analysis of the historical data of the generation side and the demand side, the uncertainty modellings of DERs and the power load are carried out, and the probability modelling for distribution system components is established. Then the system states can be generated, and the microgrid formation model for load restoration is established based on mixed integer linear programming (MILP). Moreover, a set of resilience indices of ADSs are defined. Then, this paper proposes an uncertain supply-demand scenario generation algorithm, and an ADS resilience assessment algorithm based on the Monte Carlo simulation (MCS) and the zone partition and minimal path search (ZPMPS) [23] to access these indices. Finally, the proposed resilience assessment algorithm is validated with a modified IEEE 123-bus feeder.

The reminder of this paper is organized as follows: Section 2 introduces the concept of resilience assessment. Section 3 introduces the resilience modelling. Section 4 presents the resilience indices and

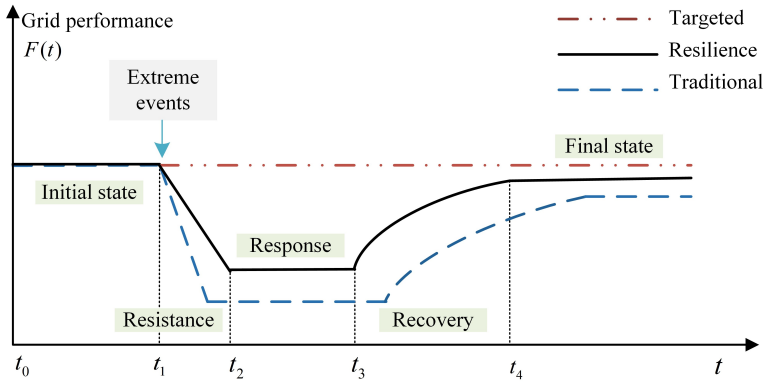

Fig. 1: Illustration of the grid resilience concept.

the algorithm of resilience assessment. Case studies and results analysis are presented in Section 5, followed by Section 6 that draws the conclusions and discusses the following work of this paper.

2 Resilience assessment conceptions

Resilience assessment is used to quantitatively measure the ability of power systems to reduce the outage consequence. In this section, the concept of resilience is firstly introduced. Then, the impact of grid-edge DERs on the resilience of ADSs is analysed. Next, the resilience assessment framework and resilience assessment modelling are introduced.

2.1 Concept of resilience

Resilience was firstly introduced by Holling in 1972 as a concept in the ecological system, which referred to "a measure of the persistence of systems and of their ability to absorb change and disturbances and still maintain the same relationships between populations or state variables" [24]. In the power system, resilience focuses on the ability of dealing with the energy supply interruption and restore critical loads under extreme events [25].

In recent years, resilience has been increasingly recognized as a design and operation goal for critical infrastructures. For utility grids, it is becoming clear that it is impossible to resist all events at all time, and strategies beyond traditional reliability study are needed to keep the lights on under extreme events. However, extreme events can cause multiple instantaneous component failures and power supply interruption, and require relatively complex restoration strategies. In these cases, the component failure rate increases sharply.

Resilience describes the process of the power system from the extreme event occurrence to the load service restoration. Notably, grid-edge DERs can improve the system resilience in all stages of disaster response, as shown in Fig. 1, where the dotted blue curve indicates the distribution system which only supplied by the source bus, and the solid black curve indicates the resilience lifting effect of the ADS with DERs.

This paper considers the microgrid formation based on grid-edge DERs. As Fig. 1 shows, we focus on the grid performance between the blue dot curve and the solid black curve, which indicates the resilience gain of the ADS brought by grid-edge DERs. Moreover, resilience assessment is used to quantitatively measure the ability of systems to reduce the outage consequence by defining a series of resilience indices. This paper focuses on the load restoration process of the distribution system after an outage (begin with t_2). The period of response and recovery are respectively measured as the decrement time of the interruption duration indices and the restored energy indices.

Notably, the resilience assessment method proposed in this paper applies to different extreme events instead of a specific extreme event. In this paper, the components parameters (the failure rate and repair rate) are set based on empirical data. If the research needs to be carried out for a specific extreme event such as typhoon or rainstorm, the components parameters can be modified according to corresponding extreme event features.

2.2 Impact of grid-edge DERs on ADS resilience

Under the energy transformation, the structure of power systems has changed rapidly. Because of the connection of the renewable DERs to distribution systems at the grid-edge, the radial topology and unidirectional flow of the traditional distribution system are completely changed, and the uncertainty of power generation of renewable DERs flows into the distribution system. At the same time, as a widespread energy resource, the DER enables the ADS to operate with a more resilient fashion and enhance the resilience of the ADS.

The effect of grid-edge DERs on the resilience of distribution systems can be analysed based on Fig. 1. We can see that the period of t_0 to t_1 is the normal operation stage of the power system. The value $F(t)$ at this stage represents the target operation state. When the extreme event occurs at t_1, the failure rates of power system components increase sharply. Then the system enters the extreme event response stage, i.e., the period of t_1 to t_2, during which the system resistants extreme events to minimize the damage of extreme events to energy infrastructures and reducing the failure loss. The period of t_2 to t_3 is the response stage, during which the system is in a state of low power supply capacity. It takes time to respond to the extreme event and prepare to restore load service. The period of t_3 to t_4 is the recover stage, during which the power supply is gradually restored to the customers. Notably, grid-edge DERs can shorten the response and recovery time by playing as backup generators after the power outage. Widely distributed in the power system, grid-edge DERs can effectively accelerate the whole restoration process by reducing the energy not supplied and the interruption duration.

2.3 Resilience assessment framework

The general resilience assessment framework of ADSs based on the sequential MCS is illustrated in Fig. 2 and introduced as follows. The whole framework is mainly consisted of five parts: data preparation, probabilistic modelling, scenario generation, scenario analysis, and resilience indices calculation.

2.3.1 Step 1. Data preparation: Data preparation denotes the process of collecting and organizing the data required to establish the probabilistic models of uncertain factors that affect reliable power supply. In this paper, uncertain factors refer to the state of system components and supply-demand scenarios. For the uncertainty of component state, the historical failure data, e.g., failure frequency and duration, of distribution system components should be prepared. For the uncertainty of supply-demand scenarios, the historial power consumption data of load nodes and the power generation of DERs,

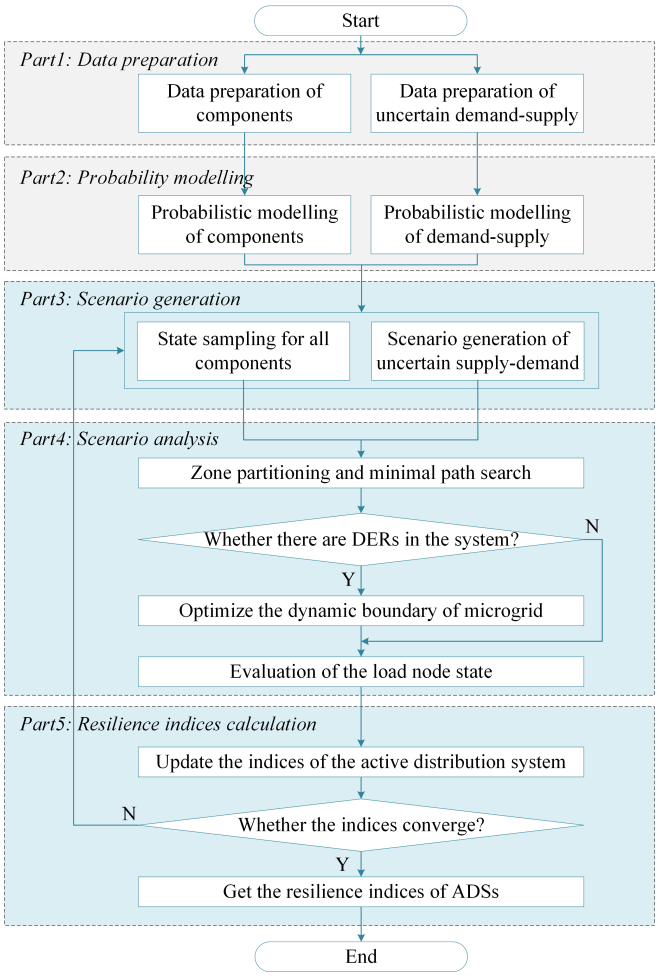

Fig. 2: Resilience assessment flowchart of active distribution systems.

e.g., wind turbines and photovoltaic units, should be prepared used to depict the probabilistic characteristics of supply-demand.

2.3.2 Step 2. Probabilistic modelling: Based on the prepared data, the reliability parameters including failure rate and repair rate can be calculated and used to establish the component state probabilistic model. In general, the component state model is used to depict the probability and duration of a component being in a normal or faulty state, and the system state can be viewed as a combination of component states. In addition, the probabilistic modelling of supply-demand uncertainty is carried out based on historical supply-demand scenarios. At the power demand side, the actual power consumption data of power users in a region for several years are selected and used to establish a demand data set. At the power supply side, this paper considers the uncertainty of power supply from wind turbines, and selects the actual wind power generation data in a region within a year to establish a supply data set. Based on these two data sets, the supply-demand model can be established by probability statistics.

2.3.3 Step 3. Scenario generation: The scenario generation for ADSs includes two parts: the supply-demand scenario generation and the system state generation. The supply-demand scenario generation is used generate the output capacity of DERs and the demand of loads, which serve as part of the analysis scenario for load restoration. According to the probability distribution characteristics of the historical supply-demand data, the supply and demand scenarios can be generated by random sampling techniques based on corresponding probability distribution models. System state scenario generation is based on MCS techniques. Specifically, the state and its duration of components are simulated one by one based on corresponding component state probabilistic models. Then, by analysing all state transition processes of components, the state transition process of the distribution system can be obtained and used in subsequent scenario analysis. The details of scenario generation based on MCS techniques are presented in Section 4.2.

2.3.4 Step 4. Scenario analysis: Uncertain supply-demand and component status together constitute the analysis scenario for resilience assessment. The aim of scenario analysis is to obtain the power supply status of load nodes in disaster scenarios, thereby determining the power outage loss of the system. To quantitatively calculate the impact of microgrid formation based on grid-edge DERs on the ADS resilience, we use a traditional distribution systems with the same topology as the ADS but without DERs as a comparison. Therefore, the resilience gain to ADSs brought by DERs can be formulated as the reduced power loss of ADSs compared to traditional distribution systems.

As shown in Fig. 2, the zone partitioning and minimal path search (ZPMPS) [23], which is a classic connectivity-based reliability scenario analysis method, is used to analyse the connectivity between load nodes and sources. In general, if there is no fault occurring in the connection between a load node and its source bus, the power supply to this load node is not affected. If there is a fault on the connection or its source bus faults, this zone where the node is located will attempt to change the power sources to DERs as a possible solution for load restoration. Details about the scenario analysis are introduced in Section 4.3. During a power outage, the distribution system operator (DSO) can deconstruct the distribution network into island microgrids by operating switchers and DERs to continue supplying the critical loads. Notably, running such bottom-up restoration strategies in parallel with traditional top-down restoration strategies (i.e., the reenergization of transmission networks using bulk generators) can effectively accelerate the load restoration process and improve power supply capability.

Notably, for a distribution system with gird-edge DERs, a MILP-based formation model of dynamic boundary microgrids is used to determine DER-based load restoration strategies. Its aim is to maximize the sum of restored critical loads while satisfying the operation constraints of both the distribution system and microgrids. On the basis, the power loss considering the impact of grid-edge DERs can be obtained. For a distribution without grid-edge DERs, the ZPMPS is sufficient for its scenario analysis.

2.3.5 Step 5. Resilience indices calculation: After extensive scenario analysis, the resilience indices can be probabilistic statistics of the power outage loss indicators in all scenarios. The definition of resilience indices is given in Section 4.1. During the MCS, resilience indices are calculated and updated iteratively. Hence the coefficient of variation (CV) can be used to determine whether the resilience assessment is converged or not. To be specific, for a resilience index, when the CV of the list formed by the index during the MCS is less than a preset value, it is considered to be converged and its assessment is stopped.

3 Resilience assessment modelling

3.1 Component state and supply-demand modelling

The two-state (i.e., normal operation and fault state) model is used to depict the state transition of distribution system components e.g. transformers, overhead lines, cables, isolating switches, fuses etc. [26], as shown in Fig. 3, where λ represents the component failure rate and μ represents the component failure repaired rate. The component state is represented by a binary value (0 for fault state and 1 for normal operation state).

Then, the time to failure (TTF) and the time to repair (TTR) of components can be generated by random sampling, as formulated in (1) and (2):

$$TTF = -\lambda^{-1} \ln \beta_1 \tag{1}$$

$$TTR = -\mu^{-1} \ln \beta_2 \tag{2}$$

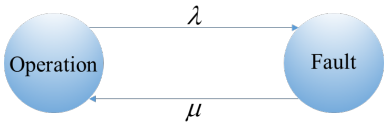

Fig. 3: Two-state component model.

where $\mu = r^{-1}$, and r represents the average repair time of the component; β_1 and β_2 are random numbers in [0, 1].

When the distribution system suffers from different types and different levels of extreme events, λ and μ need to be adjusted according to the impact of a specific extreme scenario on system components. Notably, this paper does not focus on a specific extreme event, but the proposed component probabilistic model is universal for the resilience assessment of ADSs under different extreme events.

By simulating and then combining the sequential state transition process of all components within a certain time span, the system state transition process can be obtained. Since load restoration strategies are related to supply-demand scenarios, it is needed to characterized the supply-demand uncertainty for the ADS resilience assessment. Based on the historical data of DERs' power generation and users' power consumption, a probabilistic model of uncertain supply-demand can be established. Historical supply-demand data is firstly Min-Max standardized, as formulated in (3) and (4), and its value is controlled between 0 and 1. Then the standardized data is equally divided into 20 sub-intervals. The number of samples in each sub-interval is counted to obtain the cumulative probability of each sub-interval. Finally, random numbers are uniformly sampled from the interval [0,1], and the random numbers are matched with the cumulative probability to obtain the output of DERs and the users' demand. By doing so, the supply-demand scenarios can be obtained. The random sampling probability distribution is consistent with the historical supply-demand data [23].

$$\hat{p} = (p_{\min} + p_{pu} \cdot (p_{\max} - p_{\min})) \cdot \frac{\hat{p}_{\max}}{p_{\max}} \tag{3}$$

$$\hat{l} = (l_{\min} + l_{pu} \cdot (l_{\max} - l_{\min})) \cdot \frac{\hat{l}_{mean}}{l_{mean}} \tag{4}$$

where $p_{\min}$, $p_{\max}$ respectively represent the minimum and maximum values of the actual wind power generation data; p_{pu} represents the Min-Max standardized wind active power; $\hat{p}$ and $\hat{p}_{\max}$ respectively represent the output power and rated capacity of wind turbines; $l_{\min}$, $l_{\max}$, l_{mean} respectively represent the minimum, maximum, and mean values of the actual load data; l_{pu} represents the Min-Max standardized load data; $\hat{l}$, $\hat{l}_{mean}$ respectively represent the load data and mean load.

3.2 Microgrid formation based on grid-edge DERs

During the load restoration process, grid-edge DERs can act as backup generators to support the power supply of critical loads through forming island microgrids. Such a microgrid formation problem is formulated as a MILP problem in this paper. With grid-edge DERs, the distribution system forms independent K microgrids by adjusting the radial topology after the failure, and the set of microgrids is denoted by $\mathcal{K}$. Each microgrid contains one grid-edge DER to control its voltage and frequency [3]. The distribution system node set is denoted by $\mathcal{N}$. The distribution system line set is denoted by $\mathcal{L}$. The set of nodes where DERs are located is denoted by $\mathcal{M}$. In addition, before the microgrid formation, the nodes that staying islanded without being connected to any microgrid will be removed from the set of nodes. These nodes can be found by searching in the undirected graph of the distribution system. Similar operations are used for lines. The node and line sets after removal are denoted as $\bar{\mathcal{N}}$ and $\bar{\mathcal{L}}$, respectively [3].

The object of microgrid formation is to maximize the total restored load, formulated as:

$$\max \sum\nolimits_{i\in\mathcal{N}} w_i \cdot \sum\nolimits_{k\in\mathcal{K}} v_{ik} \cdot p_i \tag{5}$$

where w_i denotes the priority weight of load i; v_{ik} is a binary variable indicating whether load i belongs to microgrid k ($v_{ik} = 1$ if node i belongs to microgrid k, and $v_{ik} = 0$ otherwise); p_i denotes the active power of load i. For the load restoration, different types of loads have different priorities. The critical loads e.g. hospitals should be prioritized to ensure power supply. Therefore, a larger value of w_i indicates a higher load priority.

The constraints for microgrid formation based on grid-edge DERs can be divided into two parts: radial topology constraints (RTCs) and system operation constraints (SOCs). The DistFlow model presented in [27] is used as the power flow model of radial distribution systems.

The RTCs are formulated as follows:

$$\sum\nolimits_{k\in\mathcal{K}} v_{ik} = 1, \forall i \in \bar{\mathcal{N}} \tag{6}$$

$$v_{ik} \le v_{jk}, \forall k \in \mathcal{K}, i \in \bar{\mathcal{N}}\backslash\{k\}, j = \theta_k(i) \tag{7}$$

$$c_{ij} = \sum_{k\in\mathcal{K}} v_{hk}, h = \zeta_k(i,j), (i,j) \in \bar{\mathcal{L}} \tag{8}$$

where (6) is used to ensure each node $i \in \bar{\mathcal{N}}$ belongs to only one microgrid. For the nodes where DREs are located, they will surely belongs to correspond to the DER, i.e., $v_{ik} = 1, i = k, \forall i \in \bar{\mathcal{N}}, i \in \mathcal{K}$. In (7), $\theta_k(i)$ is the parent node of node i regarding microgrid k, and (7) indicates that in a radial distribution system, one node can belong to microgrid k only if its parent node for this microgrid belongs to microgrid k. In (8), c_{ij} is a binary decision variables indicating whether the switch associated with line (i,j) is open ($c_{ij} = 0$) or closed ($c_{ij} = 1$), and $\zeta_k(i,j)$ denotes the children node of line (i,j) regrading microgrid k. Hence (8) denotes that the switch on this line (if it exists) should be in the closed state if line (i,j) belongs to any microgrid in $\mathcal{K}$. Note that during the scenario analysis, some lines may be at fault, i.e., the lines are in the open or closed state, which is formulated as: $c_{ij} = 0, \forall (i,j) \in \mathcal{L}_O$ and $c_{ij} = 1, \forall (i,j) \in \mathcal{L}_C$, where $\mathcal{L}_O$ and $\mathcal{L}_C$ denote the set of lines that are open and closed due to faults, respectively.

The SOCs are formulated as follows:

$$\sum\nolimits_{j\in S_i^k} P_j^k = P_i^k - v_{ik} \cdot p_i, \forall k \in \mathcal{K}, i \in \bar{\mathcal{N}} \tag{9}$$

$$\sum\nolimits_{j\in S_i^k} Q_j^k = Q_i^k - v_{ik} \cdot q_i, \forall k \in \mathcal{K}, i \in \bar{\mathcal{N}} \tag{10}$$

$$0 \le P_i^k \le v_{ik} \cdot P_k^{\max}, \forall k \in \mathcal{K}, i \in \bar{\mathcal{N}} \tag{11}$$

$$0 \le Q_i^k \le v_{ik} \cdot Q_k^{\max}, \forall k \in \mathcal{K}, i \in \bar{\mathcal{N}} \tag{12}$$

$$V_i^k = V_j^k - \frac{r_i P_i^k + x_i Q_i^k}{V_0^k} - \delta_i^k, j = \theta_k(i), i \in \bar{\mathcal{N}}\backslash\{k\}, k \in \mathcal{K} \tag{13}$$

$$0 \le V_i^k \le v_{ik} \cdot V_0^k, \forall k \in \mathcal{K}, i \in \bar{\mathcal{N}} \tag{14}$$

$$0 \le \delta_i^k \le (1 - v_{ik}) \cdot V_0^k, \forall k \in \mathcal{K}, i \in \bar{\mathcal{N}} \tag{15}$$

$$V_R - \epsilon \cdot V_R \le \sum_{k\in\mathcal{K}} V_i^k \le V_R + \epsilon \cdot V_R, \forall i \in \bar{\mathcal{N}} \tag{16}$$

where S_i^k denotes the set of children nodes of node i for microgrid k; P_i^k and Q_i^k denotes the active power and reactive power of node i in microgrid k, respectively; $P_k^{\max}$, $Q_k^{\max}$ represent to the power generation capacity of the DER in microgrid k. Equations (11) and (12) indicate that if node i does not belong to microgrid k, the real and reactive in-flow power regarding microgrid k should be zero. The voltage at the root node of the microgrid is set as the reference value

Table 1 Resilience indices for active distribution systems.

System Resilience Indices	Definition
$EER = \sum_{i\in\mathcal{N}} \dot{D}_i L_{a,i}$	Expected energy restored (EER) indicates the mathematical expectation of the energy restored after system outages during a certain period, kWh/yr.
$EITD = \sum_{i\in\mathcal{N}} \dot{D}_i N_i$	Expected interruption time decrement (EITD) indicates the mathematical expectation of the reduced interruption time after system outages during a certain period, cust.hr/yr.
$ASIFD = \frac{\sum_{i\in\mathcal{N}} \dot{\lambda}_i N_i}{\sum_{i\in\mathcal{N}} N_i}$	Average system interruption frequency decrement (ASIFD) indicates the average reduction of the customer power interruption frequency of the system during a certain period, f/cust./yr.
$ASRE = \frac{\sum_{i\in\mathcal{N}} \dot{D}_i L_{a,i}}{\sum_{i\in\mathcal{N}} N_i}$	Average system energy restored (ASER) indicates the average customer energy restored after system outages of the system during a certain period, kWh/cust./yr.
$ASITD = \frac{\sum_{i\in\mathcal{N}} \dot{D}_i N_i}{\sum_{i\in\mathcal{N}} N_i}$	Average system interruption time decrement (ASITD) indicates the average reduction in customer outage duration after system outages of the system during a certain period, hr/cust./yr.
$ACIFD = \frac{\sum_{i\in\mathcal{N}} \dot{\lambda}_i N_i}{\sum_{i\in\mathcal{N}_\Omega} N_i}$	Average customer interruption frequency decrement (ACIFD) indicates the average reduction of the interrupted customer power interruption frequency during a certain period, f/cust./yr.
$ACIDD = \frac{\sum_{i\in\mathcal{N}} \dot{D}_i N_i}{\sum_{i\in\mathcal{N}} \lambda_i N_i}$	Average customer interruption duration decrement (ACIDD) indicates the average reduction of the interrupted customer outage duration after system outages during a certain period, hr/cust./yr.

V_0^k. The voltage of other nodes in microgrid k can be solved by the DistFlow model, as formulate in (13), where r_i and x_i denote the resistance and reactance of the branch (i, j); V_i^k denotes the voltage at node i regarding microgrid k, and (14) denotes that V_i^k should be less than V_0^k if node i belongs to microgrid k, $v_{ik} = 1$. The δ_i^k in (13) is a slack variable to make the equality constraint when node i does not belongs to the microgrid k, but its parent node j belongs to microgrid k. The constraints for δ_i^k are written as (15). Moreover, equation (16) denotes that the voltage should be within a range specified by the rated voltage V_R and tolerance ϵ.

4 Resilience indices and algorithms

In this section, the resilience indices of ADSs are proposed from three perspectives: energy not supplied, power interruption time, and power interruption frequency. The resilience assessment algorithm includes two parts: scenario generation algorithm and scenario analysis algorithm.

4.1 Resilience indices

Resilience indices of ADSs are classified into load node indices and system indices. Load node indices describe the resilience of the individual load node, while system indices describe the resilience of the whole distribution system. Load node indices includes: decrement for load node average outage duration $\dot{D}_i$ (hr/yr); decrement for load node average outage frequency $\dot{\lambda}_i$ (f/yr); decrement for load node average duration of a singe outage $\dot{r}_i$ (hr).

This paper defines seven system resilience indices including expected energy restored (EER), expected interruption time decrement (EITD), average system interruption frequency decrement (ASIFD), average system energy restored (ASER), average system interruption time decrement (ASITD), average customer interruption frequency decrement (ACIFD), average customer interruption duration decrement (ACIDD). As shown in Table 1, the formulation and definition of resilience indices are expressed in detailed, where $\dot{D}_i = D_i - \hat{D}_i$, $\dot{\lambda}_i = \lambda_i - \hat{\lambda}_i$, $\dot{r}_i = r_i - \hat{r}_i$, and $\hat{D}_i$, $\hat{\lambda}_i$, $\hat{r}_i$, D_i, λ_i, r_i respectively indicate the average annual outage duration, failure probability and average outage duration of the *i*-th load node for per system outage of active distribution system and passive distribution system. L_i, N_i respectively indicate the average load and customer number of the *i*-th load node, $\mathcal{N}_\Omega$ indicates the set of load nodes affected by power interruption.

4.2 Scenario generation algorithm

The resilience scenario of the ADS is a combination of uncertain factors that affects the system resilience. In the traditional resilience assessment, the uncertain factor mainly refers to the state of vulnerable components. For ADSs, the impact of the uncertain supply-demand should be considered in the resilience assessment. The resilience scenario in this section is composed of three types of uncertain factors: vulnerable component states, uncertain DER output and uncertain load demand, formulated as follows:

$$S = \{s_c, s_g, s_l | c \in \Omega_c, g \in \Omega_g, l \in \Omega_l\} \tag{17}$$

where S represents the resilience scenario; s_c, s_g, and s_l respectively represent the state of distribution system components c, the output power state of new energy units g, and the power demand of loads l; Ω_c, Ω_g, and Ω_l respectively represent the set of distribution system components, the set of wind turbines and the set of load nodes respectively. In the scenario generation process, the state of system components are characterized by a two-state model, and $s_c \in \{0, 1\}$ ($s_c = 1$ if the component works normally and $s_c = 0$ if it malfunctions). The state change moment for each component in the given time span is:

$$T_{i,n} = \sum_{s=1}^{n} D_{i,s}, i = 1, 2, \cdots, N_C, \quad n = 1, 2, \cdots, N_{S,i} \tag{18}$$

$$T_{i,N_{S,i-1}} < T_S < T_{i,N_{S,i}}, \quad i = 1, 2, \cdots, N_C \tag{19}$$

where $T_{i,n}$ denotes the moment when component i changes state for the n-th time; $D_{i,s}$ denotes the state duration of component i in the s-th sample, generated based on (1) and (2); N_C is the number of components; $N_{S,i}$ is the number of samples for component i, which subjects to (19) where T_S denotes the total simulation time.

Then, the chronological state transition process for all components can be obtained. On this basis, the system state consists of the state of all components that can be determined according to the sequence of component state changes [26]. The scenario generation algorithm is shown in Algorithm 1. Based on the MCS framework, the state and state duration of components are firstly generated, followed by the determination of system states and their duration. Then, the load demand and DER's power generation are matched for each simulated system state. This paper stipulates the time scale of scenario analysis is the minimum time unit of the sequential change of state quantity, and the supply-demand parameters will not change during the duration of system state scenarios.

After the ADS scenario is obtained, the microgrid formation based on DERs can be solved using the MILP model built in Section 3.2 to get the post-disaster load restoration strategies. Then, the resilience indices of the ADS can be calculated according to the load restoration results.

4.3 Scenario analysis algorithm

Because DERs as flexible generators make the power flow direction of distribution systems no longer unidirectional, the traditional

Algorithm 1 scenario generation

All components are at the normal operation state;
Set $t = 0$ and scenario counter $n_s = 0$;
The initial state duration of all elements is obtained by sampling $\{T_{c,n_s}|c \in \Omega_c\}$;
while the resilience indices do not converge and $t < T_{\max}$ **do**
  Get the system state $\{s_{c,n_s}|c \in \Omega_c\}$ and the duration $D_{n_s} = \min\{T_{c,n_s}\}$;
  Generate the supply scenario $\{s_{g,n_s}|g \in \Omega_g\}$ and demand scenario $\{s_{l,n_s}|l \in \Omega_l\}$;
  Get the ADS scenarios S, perform system states analysis, determine the power supply state of each load node;
  Calculate the resilience indices;
  $t = t + D_{n_s}$;
  $n_s = n_s + 1$;
  for $c \in \Omega_c$ **do**
    if $T_{c,n_s} \neq D_{n_s-1}$ **then**
      $T_{c,n_s} = T_{c,n_s-1} - D_{n_s-1}$;
    else
      The new state duration is sampled T_{c,n_s};
    end if
  end for
end while

state analysis methods based on topology connectivity are difficult to meet the needs of scenario analysis for ADSs. Therefore, for every scenario of the ADS generated during the MCS, the scenario analysis considering DER-based load restoration is required to obtain the outage results. This paper integrates the MILP-based microgrid formation model with the ZPMPS, and propose an ADS scenario analysis algorithm as shown in Algorithm 2.

Based on the load restoration results, each energy supply path of microgrids are determined for each load node according to these rules: the low-voltage side buses of substations are the preferred choices for load power supply, followed by the DERs. According to the load node state changes before and after an outage, the fault type of load nodes can be obtained. As shown in Algorithm 2, there are six fault types for load nodes. Type I: the load node is originally in the power supplied state and not affected by the outage, meaning that is continues to be in the power supplied state. Type II: the load node is affected by the outage but can be restored after the fault isolation, and the load node continues to be in the power supplied state. Type III: the load node is originally in the power supplied state and affected by the outage, and can be restored after changing the energy supply path. Type IV: the load node is originally in the power supplied state, but loses its power supply path due to the outage, then its state transfers to the power outage state. Type V: the load node is originally in the power outage state, but after the fault is repaired, it can be restored and its state transfers to the power supplied state. Type VI: the load node is originally in the power outage state and continues to be in the power outage state.

According to the fault type of load nodes, the interruption frequency and duration can be obtained. Combined with the static parameters mentioned in Table 1 e.g. the average load and customer number for each load node, the resilience indices of load nodes and the distribution system can be calculated through statistics.

5 Cases studies

In this section, the IEEE 123-bus feeder [28] is adopted as the test system to verify the effectiveness of our proposed method. A brief description of this test system is given in Section 5.1.1. The programming environment is configured as Python 3.8.12. The microgrid formation MILP model solved with MATLAB 2021a and CPLEX 12.8.0. In addition, all the experiments were performed on a personal computer with Intel(R) Core (TM) i7-10700F CPU at 2.90 GHz and 16.00 GB RAM.

Algorithm 2 scenario analysis

Check the power supply states of each load node;
Check the power supply sources of each load node;
Determine the fault result based on the ZPMPS;
According to the built MILP model, the topology reconstruction of the microgrid;
Determine the status of the current load node and its power supply;
if random faults result in the loss of power supply to the main network in some areas, but the DER exists in the area **then**
  Determine the dynamic boundary of microgrid;
  Determine the status of the current load node and its power supply;
  for $i = 1, ..., N_{load}$ (i.e., the number of loads) **do**
    if the load was in a state of power failure originally **then**
      if the load is supplied currently **then**
        Result type V;
      else
        Result type VI;
      end if
    else
      if the power supply does not change **then**
        if the faulty component is not in the zone minimal path **then**
          Result type I;
        else
          Result type II;
        end if
      else
        if power supplied by a DER **then**
          Result type III;
        else
          Result type IV;
        end if
      end if
    end if
  end for
else
  Determining the result type by ZPMPS;
end if
Output status assessment results.

5.1 Test system introduction

5.1.1 IEEE 123-bus feeder: The standard IEEE 123-bus feeder does not include DERs, which is used as a comparison to get the resilience gain of DERs. The topology of the modified IEEE 123-bus feeder is shown as Fig. 4, where nodes 17, 250, 39, 66, 71, 96, 114, and 151 are set to DER nodes. The power generation capacity of the DER (distributed wind turbine generator) is 0.4MW and 0.3MVar. The uncertainty on the power supply side comes from the random fault of public grid and the random output of distributed wind turbines. The random fault of the public grid only considers the fault of distribution lines. The line failure rate is set to 0.1(f/yr/km), and the mean repair time is set to 5 hours. In addition, the line length, loads and power flow calculation parameters are consistent with the standard test system. The number of customers at each load node is set to 10. This distribution system can be divided into five zones based on the locations of circuit breakers. Table 2 lists the number of nodes in each zone.

5.1.2 Supply-demand data: The wind power generation data comes from the actual data of a region in China, with a sampling interval of 30 minutes. After the Min-Max standardization, the output data of DERs in the test system can be obtained by conversion according to the capacity. The conversion formula is shown (3). Load data comes from the Low Carbon London (LCL) project, which collected smart meter data from 5,567 London households between November 2011 and February 2014. This dataset contains energy consumption data with kWh, 30-minute sampling interval, unique

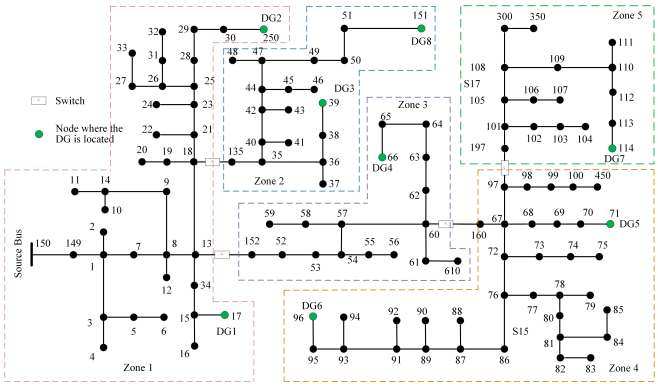

Fig. 4: Modified IEEE 123-bus feeder.

Table 2 IEEE 123-bus feeder zone partitional.

Zone	Load nodes
1	149, 1-34, 350
2	135, 35-51, 151
3	152, 52-66, 610
4	160, 67-100, 450
5	197, 101-114, 300

user IDs, date, and time. All users are divided into 16 groups according to different economic levels. Based on this, all the users are further divided into 200 groups. The load data of the LCL project in 2013 is used in this paper, and the conversion relationship between the actual load data and the load data in oue test system is shown in (4). It can be seen from Table 2, some nodes are not loaded in the IEEE 123-bus feeder. For those nodes, the average node load is considered to be zero. The modified IEEE 123-bus feeder has a total of 125 load nodes and 8 DER nodes of distributed wind turbines. After the Min-Max standardized processing of supply and demand data, 8 groups of actual wind power generation data are selected to correspond to 8 distributed wind turbines, and 125 groups of the actual load data are selected to correspond to 125 load nodes.

5.2 Resilience of the distribution system

The coefficient of variation (CV) of the EER is used as an indicator to determine whether the assessment is converged or not. In specific, the assessment is viewed as converged when the CV of the EER is less than 0.05, and not converged otherwise. In addition, a maximum simulation time that is 10,000 years is set to avoid overlong simulations, which means that the evaluation will stop when the simulation time reaches the maximum simulation time even the CV of the EER is larger than 0.05. In this situation, whether the MCS-based resilience assessment is accurate should be manually determined.

The resilience indices calculated in this paper include EER, EITD, ASRE, ASIFD, ASITD, and ACIDD (see Table 1). The resilience assessment results of the ADS are shown in Table 3. The data in the table indicate that DER effectively improves the system resilience in the distribution system, especially in the power distribution system to restore power supply energy and shorten the interruption time for load nodes. The resilience improvement is obviously reflected in EER, EITD, ASRE, ASITD, and ACIDD.

As shown in Fig. 5, the resilience improvement proportion of EER, EITD, ASRE, ASITD, and ACIDD are 36%, 41%, 36%, 41%, 38%, respectively, which all account for about 40%. The series of bars in Fig. 5 depict the proportion of load restoration effect played by DERs in the ADS. Through the microgrid formation, the DER-based load restoration effect is reflected in power supplied indices, power interruption time indices and fault frequency indices. Represented as Fig. 5, the complete bars indicate the impact of power outages, while the highlighted parts represent the quantified proportion of load restoration through the microgrid formation based on grid-edge DERs in ADSs. However, the resilience improvement is not obvious in the index that describes the decrement of interruption frequency, i.e., ASIFD. The improvement proportion in terms of the system interruption frequency is only 5%, as shown in Fig. 5. Because the DER can only flexibly adjust power supply paths by optimizing the microgrid formation, to improve the load restoration capacity of distribution systems and reduce the user's power shortage and interruption time, but rarely reduce the component failure frequency since these adjustments also cause short blackouts for nodes that need to switch power supply paths. Therefore, the DER has little influence on the improvement of the distribution system resilience in terms of the interruption frequency.

5.3 Resilience of zones and nodes

Based on the decrement of the average annual outage time of load nodes, i.e., $\dot{D}_i$ (hr/yr), this paper measures the resilience of load nodes in ADSs, as shown in Table 4. This paper does not consider the resilience of distribution system nodes without load, and sets the resilience indices of these nodes to zero. At the same time, these load node are not mentioned in Table 4. In addition, the resilience of distribution zones is analysed. Distribution system load nodes are divided into five zones according to the locations of circuit breakers, as shown in Fig. 4.

The resilience of load nodes in each zone has certain correlation. In Table 5, the average resilience indices of load nodes of the distribution system in different zones are provided. The average values of resilience indices of load nodes in different zones are obviously different. This is related to the location of the zone relative to the power supply in the distribution system. For zone 1, its nodes are close to the source bus, and the resilience of load nodes is mainly affected by the source bus, and the load restoration effect of DERs is not dominant. Zone 4 and 5, located at the grid-edge of the distribution system, are far away from the source bus. There are DERs in these two zones. The load restoration effect of DERs is significant. Hence these load nodes have stronger resilience capacity. Fig. 6 depicts the resilience index of each load node (decrement for load node average annual outage duration $\dot{D}_i$ (hr/yr)) in the distribution system in the form of a bar chart. Load nodes in different zones are highlighted in different colours in the bar chart. There is a similar resilience pattern for load nodes in the same zone. The loads far away from the source bus and close to the grid-edge DER node in the region has a better resilience level. The load nodes close to the source bus have weak load restoration capacity. As the topology position is close to the end of the distribution network and the DER node, the load restoration capacity is gradually enhanced.

Fig. 7 describes the resilience index of load nodes (decrement for load node average annual outage duration $\dot{D}_i$ (hr/yr)) by the colour of load nodes. In this figure, the nodes with no loads are represented as white circles with black edge, e.g., the load node 3, 8, and 13. The DER nodes are denoted by blue edge nodes (i.e., nodes 17, 250, 39, 66, 71, 96, 114, and 151). The darker the green color for the load node in the figure, the larger the $\dot{D}_i$, which means the stronger the resilience of these load nodes.

As shown in Fig. 7, it is not difficult to find that the resilience of load nodes is closely related to the position of DERs in the distribution system topology. The stronger the power supply restoration capability of the load nodes near the grid-edge DER, the higher their resilience, e.g., the DER nodes 71, 96, and 114. This is consistent with our conclusion in Fig. 6. The load restoration effect of load nodes near the source bus is not obvious. The power supply restoration of such nodes is mainly affected by the source bus. For the nodes far away from the source bus, the nodes at the grid-edge of the distribution system, their load restoration effect is better. The load nodes in the same branch as DER nodes or DER nodes themselves have the best restoration effect and higher resilience capacity. These nodes are less affected by the fault of the source bus, because they are closer to the grid-edge DERs, so these nodes have strong load restoration capacity and better resilience indices.

Table 3 Active distribution system resilience indices.

EER (kWh/yr)	EITD (cust.hr/yr)	ASRE (kWh/cust./yr)	ASIFD (f/cust./yr)	ASITD (hr/cust./yr)	ACIDD (hr/cust./yr)
786.1	212.2	0.6289	0.003899	0.1698	1.915

Table 4 Active distribution system load nodes resilience indices.

Load nodes	$\dot{D}_i$ (hr/yr)	$\dot{\lambda}_i$ (f/yr.)	$\dot{r}_i$ (hr)	Load nodes	$\dot{D}_i$ (hr/yr)	$\dot{\lambda}_i$ (f/yr.)	$\dot{r}_i$ (hr)
Zone 1				59	0.1851	-0.000159	2.006
1	0.0283	0.002506	1.401	60	0.2170	-0.000289	2.129
2	0.0248	0.000149	1.305	62	0.2548	-0.000517	2.357
4	0.0068	0.002914	-0.300	63	0.2580	-0.000611	2.289
5	0.0115	0.002296	0.016	64	0.3420	-0.000516	2.762
6	0.0101	-0.000759	0.330	65	0.1449	-0.030389	1.813
7	0.0186	0.001083	0.644	66	0.4980	0.094054	0.135
9	0.0003	-0.000492	0.086	Zone 4			
10	0.0004	-0.001633	0.158	68	0.2798	-0.002797	2.264
11	-0.0029	-0.001633	0.099	69	0.3521	-0.003782	2.655
12	0.0238	0.002306	0.369	70	0.3112	-0.007137	2.281
16	0.0587	0.002845	0.879	71	0.4655	0.086460	0.243
17	0.1233	0.021110	0.457	73	0.2861	-0.003665	2.167
19	0.1420	0.004195	1.903	74	0.2918	-0.000296	1.976
20	0.1486	0.002931	1.751	75	0.2242	-0.002085	1.449
22	0.1552	-0.001097	1.853	76	0.3679	-0.002860	0.208
24	0.1583	-0.003220	1.827	77	0.3688	-0.004008	2.584
28	0.2469	0.001559	2.673	79	0.2269	-0.003933	1.545
29	0.2893	0.004587	2.777	80	0.2168	-0.006094	1.460
30	0.3330	0.005820	2.823	82	0.2500	-0.004382	1.469
31	0.1886	0.002879	1.739	83	0.2626	-0.004280	1.476
32	0.1915	0.002846	1.621	84	0.1730	-0.003847	0.960
33	0.2231	0.006502	1.713	85	0.2481	-0.005305	1.280
34	0.0402	0.001301	0.846	86	0.3516	-0.003916	2.362
Zone 2				87	0.4200	-0.003945	2.580
35	0.1947	0.002572	2.343	88	0.3988	-0.004778	2.402
37	0.2880	0.003602	2.551	90	0.3824	-0.002750	2.160
38	0.3236	0.005244	2.839	92	0.5030	-0.002666	2.670
39	0.4273	0.079851	0.281	94	0.4899	-0.005758	2.523
41	0.2089	0.005664	1.957	95	0.4707	-0.009264	2.448
42	0.2102	0.004815	2.091	96	0.6177	0.121356	0.135
43	0.2517	0.005224	2.191	98	0.2497	-0.002023	1.863
45	0.2525	0.005893	2.204	99	0.1824	-0.001408	1.208
46	0.2510	0.005043	2.066	100	0.3255	-0.001965	2.010
47	0.2158	0.003447	1.873	Zone 5			
48	0.1129	0.005509	0.789	102	0.3061	-0.003132	2.118
49	0.2112	0.001693	1.771	103	0.4057	-0.002571	2.590
50	0.3198	-0.000168	2.608	104	0.3845	-0.003810	2.192
51	0.3459	0.002616	2.621	106	0.3548	-0.004651	2.334
Zone 3				107	0.3444	-0.003298	2.023
52	0.0948	0.001371	1.551	109	0.4197	-0.000773	2.411
53	0.1182	-0.000082	1.869	111	0.4232	-0.002884	2.179
55	0.0943	0.000344	1.234	112	0.456	-0.001785	2.479
56	0.1213	0.002322	1.317	113	0.5612	-0.001377	2.818
58	0.1501	-0.001670	1.810	114	0.6918	0.142964	-0.150

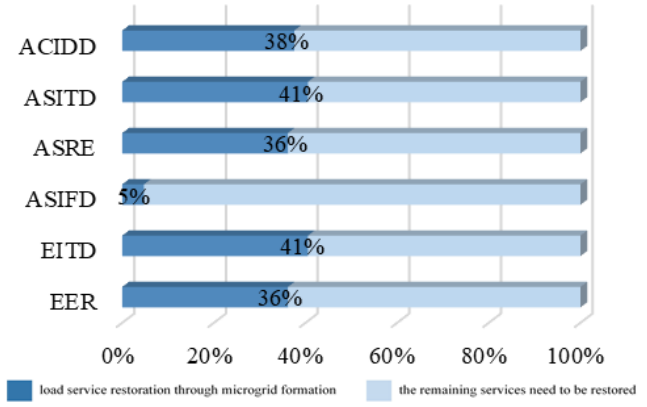

Fig. 5: The improvement proportion of microgrid formation for load service restoration.

Table 5 Average for distribution system load nodes resilience indices.

Zones	Avg ($\dot{D}_i$)	Avg ($\dot{\lambda}_i$)	Avg ($\dot{r}_i$)
1	0.1052	0.002565	1.172
2	0.2581	0.009358	0.009358
3	0.1800	-0.002745	1.922
4	0.3282	0.007738	1.723
5	0.4347	0.011868	2.099

6 Conclusions

This paper proposes a resilience assessment method of ADSs considering the microgrid formation based on grid-edge DERs. The proposed method is helpful to solve the problems brought by the integration of grid-edge DERs on the resilience assessment of distribution systems. Firstly, the uncertainty modelling of ADSs is carried out, and the analysis scenario of ADSs is defined consisting of the vulnerable components state and uncertain supply-demand. Then, the scenario generation and analysis algorithms of ADSs are proposed. In the scenario analysis algorithm, the microgrid formation model is established and integrated with the ZPMPS. In addition, a set of resilience indices are proposed and calculated based the sequential MCS. Finally, a modified IEEE 123-bus feeder is used to verify the effectiveness of the proposed method, which shows

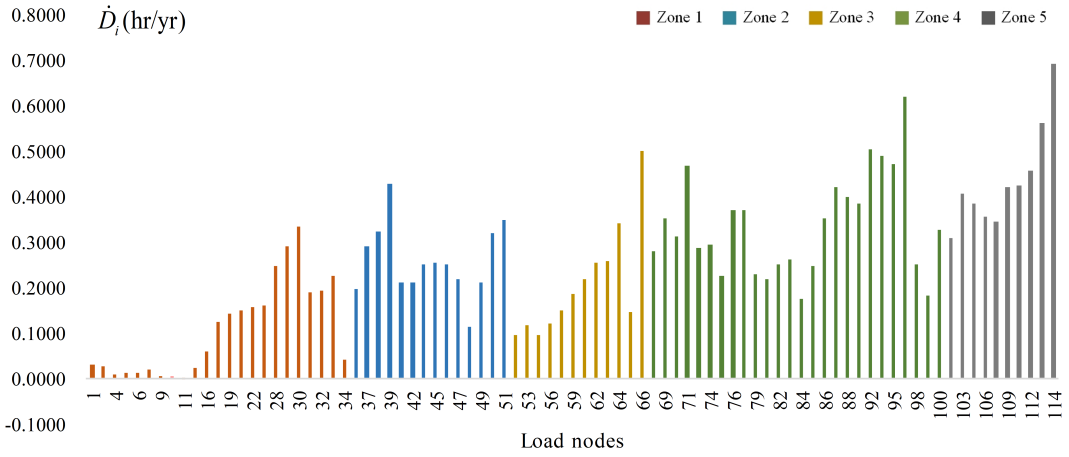

Fig. 6: Bar chart for active distribution system load nodes resilience.

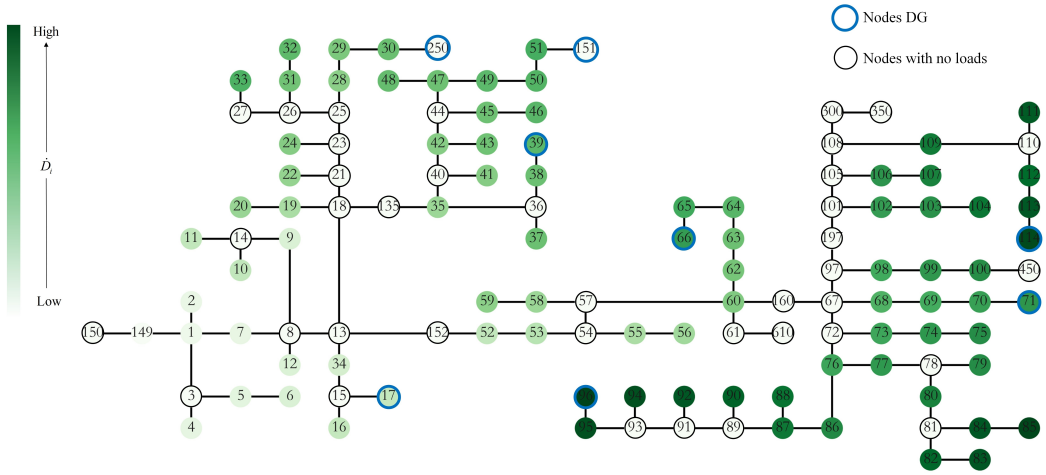

Fig. 7: Active distribution system load nodes resilience.

that DERs can efficiently improve the resilience and load restoration capacity of ADSs from multi perspectives.

In the future, the influence of extreme events on the output of DERs and the component resilience parameters e.g. failure rate and repair time deserve is worth studying.

7 Acknowledgments

This work was supported in part by the National Natural Science Foundation of China (52222705).

References

8 References

1 Mishra, D.K., Ghadi, M.J., Azizivahed, A., Li, L., Zhang, J.: 'A review on resilience studies in active distribution systems', *Renewable and Sustainable Energy Reviews*, 2021, **135**, pp. 110201

2 Bie, Z., Lin, Y., Li, G., Li, F.: 'Battling the extreme: A study on the power system resilience', *Proceedings of the IEEE*, 2017, **105**, (7), pp. 1253–1266

3 Chen, C., Wang, J., Qiu, F., Zhao, D.: 'Resilient distribution system by microgrids formation after natural disasters', *IEEE Transactions on smart grid*, 2015, **7**, (2), pp. 958–966

4 Panteli, M., Mancarella, P.: 'Influence of extreme weather and climate change on the resilience of power systems: Impacts and possible mitigation strategies', *Electric Power Systems Research*, 2015, **127**, pp. 259–270

5 Ton, D.T., Wang, W.P.: 'A more resilient grid: The us department of energy joins with stakeholders in an r&d plan', *IEEE Power and Energy Magazine*, 2015, **13**, (3), pp. 26–34

6 Hussain, A., Arif, S.M., Aslam, M., Shah, S.D.A.: 'Optimal siting and sizing of tri-generation equipment for developing an autonomous community microgrid considering uncertainties', *Sustainable Cities and Society*, 2017, **32**, pp. 318–330

7 Gao, H., Chen, Y., Xu, Y., Liu, C.C.: 'Resilience-oriented critical load restoration using microgrids in distribution systems', *IEEE Transactions on Smart Grid*, 2016, **7**, (6), pp. 2837–2848

8 Gilani, M.A., Kazemi, A., Ghasemi, M.: 'Distribution system resilience enhancement by microgrid formation considering distributed energy resources', *Energy*, 2020, **191**, pp. 116442

9 Panteli, M., Trakas, D.N., Mancarella, P., Hatziargyriou, N.D.: 'Power systems resilience assessment: Hardening and smart operational enhancement strategies', *Proceedings of the IEEE*, 2017, **105**, (7), pp. 1202–1213

10 Wang, Z., Wang, J.: 'Self-healing resilient distribution systems based on sectionalization into microgrids', *IEEE Transactions on Power Systems*, 2015, **30**, (6), pp. 3139–3149

11 Hussain, A., Bui, V.H., Kim, H.M.: 'Microgrids as a resilience resource and strategies used by microgrids for enhancing resilience', *Applied energy*, 2019, **240**, pp. 56–72

12 Kim, J., Dvorkin, Y.: 'Enhancing distribution system resilience with mobile energy storage and microgrids', *IEEE Transactions on Smart Grid*, 2018, **10**, (5), pp. 4996–5006

13 Sedzro, K.S.A., Lamadrid, A.J., Zuluaga, L.F.: 'Allocation of resources using a microgrid formation approach for resilient electric grids', *IEEE Transactions on Power Systems*, 2017, **33**, (3), pp. 2633–2643

14 Bian, Y., Chen, C., Huang, Y., Bie, Z., Catalao, J.P.: 'Service restoration for resilient distribution systems coordinated with damage assessment', *IEEE Transactions on Power Systems*, 2022, **37**, (5), pp. 3792–3804

15 Huang, Y., Li, G., Chen, C., Bian, Y., Qian, T., Bie, Z.: 'Resilient distribution networks by microgrid formation using deep reinforcement learning', *IEEE Transactions on Smart Grid*, 2022, **13**, (6), pp. 4918–4930
16 Carlson, J., Haffenden, R., Bassett, G., Buehring, W., Collins.III, M., Folga, S., et al. 'Resilience: Theory and application'. Argonne National Lab.(ANL), Argonne, IL (United States), 2012.
17 Roege, P.E., Collier, Z.A., Mancillas, J., McDonagh, J.A., Linkov, I.: 'Metrics for energy resilience', *Energy Policy*, 2014, **72**, pp. 249–256
18 Watson, J.P., Guttromson, R., Silva.Monroy, C., Jeffers, R., Jones, K., Ellison, J., et al.: 'Conceptual framework for developing resilience metrics for the electricity oil and gas sectors in the united states', *Sandia national laboratories, albuquerque, nm (united states), tech rep*, 2014,
19 Shinozuka, M., Chang, S.E., Cheng, T.C., Feng, M., O'rourke, T.D., Saadeghvaziri, M.A., et al.: 'Resilience of integrated power and water systems'. (Citeseer, 2004)
20 Chanda, S., Srivastava, A.K.: 'Defining and enabling resiliency of electric distribution systems with multiple microgrids', *IEEE Transactions on Smart Grid*, 2016, **7**, (6), pp. 2859–2868
21 Maliszewski, P.J., Perrings, C.: 'Factors in the resilience of electrical power distribution infrastructures', *Applied Geography*, 2012, **32**, (2), pp. 668–679
22 Reed, D.A., Kapur, K.C., Christie, R.D.: 'Methodology for assessing the resilience of networked infrastructure', *IEEE Systems Journal*, 2009, **3**, (2), pp. 174–180
23 Bie, Z., Zhang, P., Li, G., Hua, B., Meehan, M., Wang, X.: 'Reliability evaluation of active distribution systems including microgrids', *IEEE Transactions on power systems*, 2012, **27**, (4), pp. 2342–2350
24 Holling, C.S.: 'Resilience and stability of ecological systems', *Annual review of ecology and systematics*, 1973, pp. 1–23
25 Bennett, J.A., Trevisan, C.N., DeCarolis, J.F., Ortiz.García, C., Pérez.Lugo, M., Etienne, B.T., et al.: 'Extending energy system modelling to include extreme weather risks and application to hurricane events in puerto rico', *Nature Energy*, 2021, **6**, (3), pp. 240–249
26 Li, G., Huang, Y., Bie, Z., Ding, T.: 'Machine-learning-based reliability evaluation framework for power distribution networks', *IET Generation, Transmission & Distribution*, 2020, **14**, (12), pp. 2282–2291
27 Yeh, H.G., Gayme, D.F., Low, S.H.: 'Adaptive var control for distribution circuits with photovoltaic generators', *IEEE Transactions on Power Systems*, 2012, **27**, (3), pp. 1656–1663
28 Schneider, K.P., Mather, B., Pal, B., Ten, C.W., Shirek, G.J., Zhu, H., et al.: 'Analytic considerations and design basis for the ieee distribution test feeders', *IEEE Transactions on power systems*, 2017, **33**, (3), pp. 3181–3188